Asociación Argentina
de Mecánica Computacional

Mecánica Computacional Vol XXXIII, págs. 1849-1860 (artículo completo)
Graciela Bertolino, Mariano Cantero, Mario Storti y Federico Teruel (Eds.)
San Carlos de Bariloche, 23-26 Setiembre 2014

EXTENDED KALMAN FILTER IDENTIFICATION FOR THE PARAMETERS OF A THREE-BLADE WIND TURBINE DYNAMICS

Fabio F. Real[a] **and Thiago G. Ritto**[b]

[a]*National Metrology, Quality and Technology Institute, INMETRO, Rio Comprido, 20251-020, Brazil, ffreal@inmetro.gov.br*
[b]*Dept. de Eng. Mecânica, Universidade Federal do Rio de Janeiro, Ilha do Fundão, 21945-97, Rio de Janeiro, Brazil, tritto@mecanica.ufrj.br*

Keywords: wind turbine dynamics, parameter identification, Bayesian filter, Extended Kalman Filter.

Abstract. Nowadays there are proposals and politics in several planet regions with targets of renewable sources adoption. In this context, wind energy presents an important source growing up in electrical energy generation, motivated by public politics and by technological maturation, being more competitive compared to conventional sources. One of actual problems in wind turbines design is parameters determination in structural calculus, which several times arise by experimental assumptions. This paper presents an application of Extended Kalman Filter (EKF) methodology for parameter identification in structural analysis of three-blade wind turbine, applying a nonlinear computational dynamical model from so-called field data.

1 INTRODUCTION

For centuries wind power has been applied for watering in agriculture by windmills. However, at the beginning of the twentieth century practically the wind power extinguished due appearance of steam machine and engines. In the 70's, due international oil crisis, wind power gains importance, consolidating after Kyoto Protocol signed in 90`s, enabling the manufacturing of wind turbine in commercial scale payable the global investments (Edenhofer, 2011).

Although only to feed about 2% of world demand, the use of wind energy for electricity production has increased about 25% annually, being more significant in Europe in countries such as Spain, Denmark and Germany. In Brazil, this energy had an increase of 80.6 % in less than three years, totaling 4.8 MW in 2013. The machine that converts wind energy into electrical energy is called wind turbine. They have two main types of wind turbine: vertical and horizontal. Vertical wind turbines have a more targeted application to urban areas due to the low noise level and power generation with any intensity of wind. However, its energy efficiency is low compared to horizontal wind turbines. Although more efficient, horizontal wind turbines depend on a minimum level of intensity of wind and its noise level is considered high, being more targeted to wind farms and offshore application.

The structural design of horizontal wind turbines depends on the determination of the stiffness and damping coefficients of that are determined by experiments. Furthermore, these parameters change over time due to the use of the equipment, the loosening of semi-rigid fixings on the bases and its components as well as change of mass and stiffness due corrosion. Therefore, identification of stiffness and damping coefficients becomes strategic and may indicate the monitoring of wind turbine structural stability and contribute to reducing the costs of field tests for its determination on projects.

For these reasons, the objective of this paper is to identify the stiffness and damping coefficients for a wind turbine with three blades, applying the recursive methods of the Extended Kalman Filter suitable for parameter identification in a non-linear mathematical model for rigid multibody from treated field data and synthetic data. Extended Kalman Filter method for identification is a low computational cost alternative, but there are restrictions on its uses.

2 MATHEMATICAL MODELING OF THE HORIZONTAL WIND TURBINE DYNAMICS

Exciting force acting on wind turbines is coming from the action of wind on the blades, on the nacelle and on the tower, as well the gravitational force exerted by this assembly. Applying the balance of linear and angular momentum, it is possible to obtain an ordinary differential equations system with the number equal to the number of degrees of freedom of this system.

The model developed here was adopted from helicopters dynamics by Gonzaga (2013), based on the dynamic equations contained in Tenenbaum (2006), which is consistent to models developed by Flowers and Tongue (1988), Robinson et al. (1997) and Saracho (2002). This model considers the tower as a concentrated mass along the nacelle, representing a rigid body. It also considers the blades as two-dimensional rigid elements with a certain eccentricity, being each blade associated with the rotor head through a point here called link distant d from origin.

Considering the basis $\hat{n}_1$ e $\hat{n}_2$ fixed in inertial frame $\Re$ and a Cartesian coordinate system with origin (O) at the geometric center of the rotor head (figure 1), when at rest position, it can write the position of the mass center of the rotor head (H*) with respect to the origin (O) of the coordinate system in function of time (t) as:

$$\boldsymbol{p}^{H*/O}(t) = \left[x(t) + e\cos(\epsilon + \Omega t)\right]\hat{n}_1 + \left[y(t) + e\,\text{sen}(\epsilon + \Omega t)\right]\hat{n}_2 \tag{1}$$

where$x(t)$ is the coordinate of the mass center of the rotor head in function of time relative to the x-axis, $y(t)$ is the coordinate of the mass center of the rotor head in function of time relative to the y-axis, e is eccentricity of the rotor head relative to the inertial coordinate system, ϵ is the angle caused by eccentricity and Ω is blade rotation.

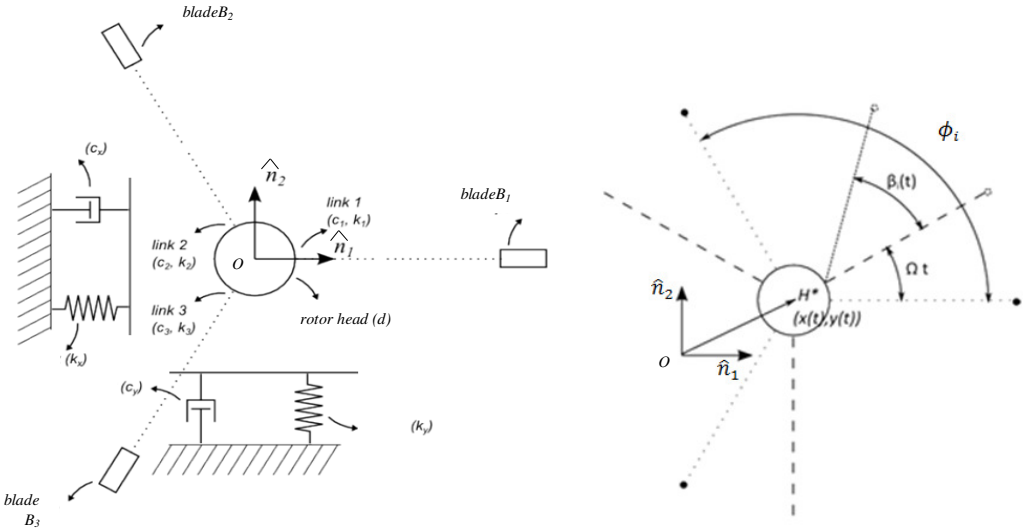

Figure 1 - Schematic representation for modeling a horizontal wind turbine.

Considering that each blade has a phase angle (ϕ_i), or azimuth, it can determine the position of the mass center blade B_i:

$$\boldsymbol{p}^{B_i*/O}(t) = \left[x(t) + d\cos(\phi_i + \Omega t) + \left(d + \frac{h_{B_i}}{2}\right)\cos\left(\phi_i + \Omega t + \beta_i(t)\right)\right]\hat{n}_1 + \left[y(t) + d\,\text{sen}(\phi_i + \Omega t) + \left(d + \frac{h_{B_i}}{2}\right)\text{sen}(\phi_i + \Omega t + \beta_i(t))\right]\hat{n}_2 \tag{2}$$

Deriving from *(1)* and *(2)* obtains the velocity of the concentrated mass in the rotor head ($\boldsymbol{v}^{\Re}_{H*}$) and the velocity related to the mass center of each blade ($\boldsymbol{v}^{\Re}_{B_i*}$).

2.1 Linear momentum balance

Linear momentum balance related to the concentrated mass of the tower with the nacelle is given by:

$$\boldsymbol{G}^{\Re}_{H} = m_H \boldsymbol{v}^{\Re}_{H*} \tag{3}$$

where m_H is concentrated mass of the tower with the nacelle.

Calculus mass m_H cannot be considered as the direct sum of the nacelle and the tower masses, because only the tower is on balance. The effective mass of the tower corresponds to the third part of its total mass. Linear momentum for each blade is given by:

$$\boldsymbol{G}_{B_i}^{\Re} = \iint_{B_i} \boldsymbol{v}_{P_i}^{\Re} dm_{B_i} \tag{4}$$

where$\boldsymbol{v}_{P_i}^{\Re}$ is velocity vector at point P_i for each blade in relation to the *link* and dm_{B_i} is infinitesimal mass element of the blade.

From the equation *(4)* and mass center definition can get linear momentum relating to each blade:

$$\boldsymbol{G}_{B_i}^{\Re} = m_{B_i} \boldsymbol{v}_{B_{i^*}}^{\Re} \tag{5}$$

wherem_{B_i} is mass of each blade. Considering equal masses of all blades, total linear momentum of the system is defined by:

$$\boldsymbol{G}_T^{\Re} = \boldsymbol{G}_H^{\Re} + \sum_{i=1}^{N} \boldsymbol{G}_{B_i}^{\Re} \tag{6}$$

$$\boldsymbol{G}_T^{\Re} = m_H \boldsymbol{v}_{H^*}^{\Re} + \sum_{i=1}^{N} (m_{B_i} \boldsymbol{v}_{B_{i^*}}^{\Re}) \tag{7}$$

$$\boldsymbol{G}_T^{\Re} = m_H \boldsymbol{v}_{H^*}^{\Re} + N m_{B_i} \sum_{i=1}^{N} \boldsymbol{v}_{B_{i^*}}^{\Re} \tag{8}$$

Applying the 2nd Newton Law, it has that:

$$\sum \boldsymbol{F}_{ext} = \dot{\boldsymbol{G}}_T^{\Re} \tag{9}$$

where$\boldsymbol{F}_{ext}$ are external forces acting on the system.

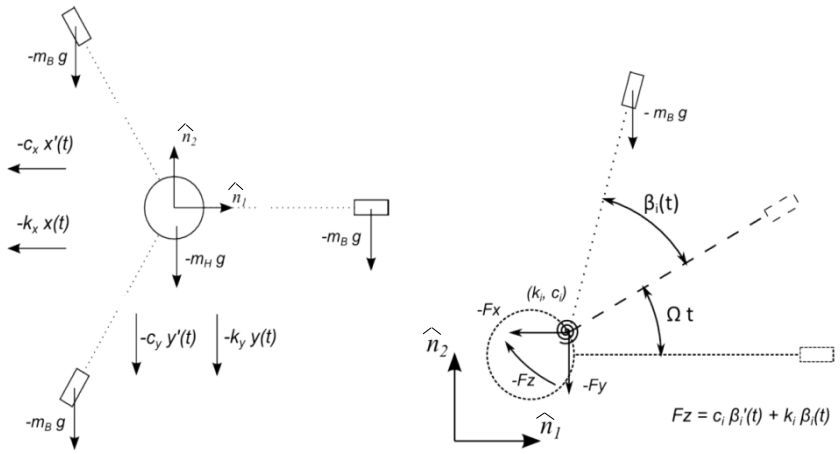

Figure 2 – Acting forces in the modeling of a horizontal wind turbine.

External forces are considered due to the action of the wind and the gravitational force. The multibody model has stiffness and damping, defined by:

$$[-c_x - \dot{x}(t) - k_x x(t)]\hat{n}_1 + \left[-c_y - \dot{y}(t) - k_y y(t) - \left(N m_{B_i} + m_H\right) g\right]\hat{n}_2 = \frac{d}{dx} \boldsymbol{G}_T^{\Re} \tag{10}$$

where$g$ is gravity acceleration, k_x is stiffness coefficient in direction $\hat{n}_1$, k_y is stiffness

coefficient in direction $\hat{n}_2$, c_x is the damping coefficient in direction$\hat{n}_1$ and c_y is the damping coefficient in direction $\hat{n}_2$.

Deriving from total linear momentum, it gets the first two equations of motion:

$$\left(Nm_{B_i}+m_H\right)\ddot{x}(t)+c_x\dot{x}(t)+k_x x(t)=em_H\Omega^2\cos(\epsilon+\Omega t)+m_{B_i}\left(d+\frac{h_{B_i}}{2}\right)\sum_{i=1}^{N}\left[\ddot{\beta}(t)sen\left(\phi_i+\Omega t+\beta_i(t)\right)+\left(\Omega+\dot{\beta}(t)\right)^2\cos\left(\phi_i+\Omega t+\beta_i(t)\right)\right] \quad (11)$$

$$\left(Nm_{B_i}+m_H\right)\ddot{y}(t)+c_y\dot{y}(t)+k_y y(t)+\left(Nm_{B_i}+m_H\right)g=em_H\Omega^2\,\mathrm{sen}(\epsilon+\Omega t)-m_{B_i}\left(d+\frac{h_{B_i}}{2}\right)\sum_{i=1}^{N}\left[\ddot{\beta}(t)cos\left(\phi_i+\Omega t+\beta_i(t)\right)-\left(\Omega+\dot{\beta}(t)\right)^2\mathrm{sen}\left(\phi_i+\Omega t+\beta_i(t)\right)\right] \quad (12)$$

2.2 Angular momentum balance

Considered system has (*N*+2) degrees of freedom for two translational degrees of freedom and *N* degrees of freedom for the blades, having the necessity to determine more *N* equations in order to be able to solve the system of non-linear equations.

Determining these non-linear equations can use the strategy of replacing the *link* for each one of the blades by the reaction forces and bend momentums. This strategy turn on possible to calculate the angular momentum balance without knowing the magnitudes of the reaction forces and bend momentums.

Angular momentum balance for one blade B_i with respect to a reference *link* point L_i can be obtained by:

$$\boldsymbol{H}^{\Re}_{B_i/L_i}=\iint_{B_i}\boldsymbol{p}^{P_i/L_i}\times\boldsymbol{v}^{\Re}_{P_i}dm_{B_i} \quad (13)$$

where$\boldsymbol{p}^{P_i/L_i}$ is position vector of a reference blade point P_i in relation to *link* point L_i and $\boldsymbol{v}^{\Re}_{P_i}$ is velocity of the point P_i of this blade, determined as

$$\boldsymbol{v}^{\Re}_{P_i}=\boldsymbol{v}^{\Re}_{L_i}+\boldsymbol{\omega}^{\Re}_{B_i}\times\boldsymbol{p}^{P_i/L_i} \quad (14)$$

where$\boldsymbol{\omega}^{\Re}_{B_i}$is angular velocity of bladeB_i contained in $\Re$ and $\boldsymbol{v}^{\Re}_{L_i}$ is velocity vector at *link* point L_i. Thus, angular momentum balance of a blade B_i can be rewritten as:

$$\boldsymbol{H}^{\Re}_{B_i/L_i}=\iint_{B_i}(\boldsymbol{p}^{P_i/L_i}\times\boldsymbol{v}^{\Re}_{P_i})dm_{B_i}+\iint_{B_i}\boldsymbol{p}^{P_i/L_i}\times(\boldsymbol{\omega}^{\Re}_{B_i}\times\boldsymbol{p}^{P_i/L_i})dm_{B_i} \quad (15)$$

From the definition of mass center and knowing that blade inertia vector in relation to *link* point L_i is defined as the product of blade inertia tensor regarding L_i with unit vector in the same direction of the angular velocity $\boldsymbol{\omega}^{\Re}_{B_i}$(in that case,$\hat{n}_3$), it can obtain the following expression for angular momentum (TENENBAUM , 2006) :

$$\boldsymbol{H}^{\Re}_{B_i/L_i}=\boldsymbol{p}^{B_i*/L_i}\times m_{B_i}\boldsymbol{v}^{\Re}_{L_i}+\boldsymbol{I}_i^{B_i/L_i}.\boldsymbol{\omega}^{\Re}_{B_i} \quad (16)$$

where$\boldsymbol{I}_i^{B_i/L_i}$ is blade inertia tensor in relation to L_i. Equation *(16)* shows an extra member (highlighted in blue). This member appears due to the fact that *link* point L_i does not coincide with the blade mass center and for being in motion ($\boldsymbol{v}^{\Re}_{L_i}\neq 0$). For this same reason, the sum of

the external bend momentums with respect to L_i ($\sum \boldsymbol{M}_{ext}{}^{L_i}$) must have an additional member (TENENBAUM , 2006):

$$\sum \boldsymbol{M}_{ext}{}^{L_i} = \dot{\boldsymbol{H}}^{\Re}_{B_i/L_i} + (\boldsymbol{v}^{\Re}_{L_i} \times \boldsymbol{G}^{\Re}_{B_i}) \tag{17}$$

Considering that the rate of blade angular momentum ($\dot{\boldsymbol{H}}^{\Re}_{B_i/L_i}$) must be obtained from inertia tensor being invariant with respect to time, it is possible to write:

$$\sum \boldsymbol{M}_{ext}{}^{L_i} = \boldsymbol{I}_i^{B_i/L_i}.\boldsymbol{\alpha}^{\Re}_{B_i} + \boldsymbol{p}^{B_i*/L_i} \times m_{B_i}\boldsymbol{a}^{\Re}_{L_i} + \boldsymbol{\omega}^{\Re}_{B_i} \times \boldsymbol{I}_i^{B_i/L_i}.\boldsymbol{\omega}^{\Re}_{B_i} + \boldsymbol{\omega}^{\Re}_{B_i} \times \boldsymbol{p}^{B_i*/L_i} \times m_{B_i}\boldsymbol{v}^{\Re}_{L_i} + (\boldsymbol{v}^{\Re}_{L_i} \times \boldsymbol{G}^{\Re}_{B_i}) \tag{18}$$

where $\boldsymbol{\alpha}^{\Re}_{B_i}$ is blade angular acceleration vector and $\boldsymbol{a}^{\Re}_{L_i}$ is the acceleration vector of *link* point L_i. The equation solution *(18)* depends on the development of the inertia tensor ($\boldsymbol{I}_i^{B_i/L_i}$). For that it can consider the blade as a parallelepiped with rectangular section in relation to its mass center, height like blade total length (h_{B_i}), width (w_{B_i}) and negligible thickness.

In the same way of equation *(10)*, the first member of equation *(18)* refers to sum of bend momentums relation to *link* point L_i ($\boldsymbol{M}_{ext}{}^{L_i}$), described for:

$$\sum \boldsymbol{M}_{ext}{}^{L_i} = \left[-c_{\beta_i}\dot{\beta}_i(t) - k_{\beta_i}\beta_i(t) - m_{B_i}g\left(d + \frac{h_{B_i}}{2}\right)\cos(\phi_i + \Omega t + \beta_i(t))\right]\hat{n}_3 \tag{19}$$

where k_{β_i} is blade stiffness coefficient (*lag*) and c_{β_i} is blade damping coefficient (*lag*).

Therefore, developing equation *(18)* and taking equation *(19)* it obtain the *N* missing equations for the solution of ordinary differential equations system:

$$\left[\frac{\left(h_{B_i}+w_{B_i}\right)^2}{12} + \left(d + \frac{h_{B_i}}{2}\right)^2\right] m_{B_i}\ddot{\beta}_i + c_{\beta_i}\dot{\beta}_i(t) + k_{\beta_i}\beta_i(t) + m_{B_i}\left(d + \frac{h_{B_i}}{2}\right) d\Omega^2 \operatorname{sen}(\beta_i(t)) + m_{B_i}g\left(d + \frac{h_{B_i}}{2}\right)\cos(\phi_i + \Omega t + \beta_i(t)) = m_{B_i}\left(d + \frac{h_{B_i}}{2}\right)\{[\ddot{x}(t)\operatorname{sen}(\phi_i + \Omega t + \beta_i(t))] - [\ddot{y}(t)\cos(\phi_i + \Omega t + \beta_i(t))]\} \tag{20}$$

The equations *(11)*, *(12)* and *(20)* for each blade form the system of ordinary differential equations and non-linear coupled to be solved numerically.

2.3 Parameter identificatoion – Extended Kalman Filter

Parameter identification determines values that minimize the difference between observed and calculated data of certain magnitudes, implying uncertainty in their results (Costa, 2006). This identification can be a sequential estimation (recursive) of the parameters of a dynamic system using a sequence of measurements with noise generated by itself (Ristic *et al*., 2004).

Among the identification methods applied for nonlinear systems have a method by analytical approach, the method of the Extended Kalman Filter. This method was originally developed to estimate the states of a system, providing dynamic responses. However, it can be used to identify parameters with appropriate adaptations.

Extended Kalman Filter is based on classic Kalman Filter with linearization at each instant of nonlinear functions. This local linearization is solved analytically and corresponds to Jacobians of functions.

This method can be applied in non-linear functions since these are continuous, with cases in which their performance is compromised when the nonlinearity of the function is very

severe (Ristic *et al.*, 2004).

Kalman Filter basis predict the following value based on the previous value. It is assumed that the domain $\mathbb{R}^N$, it observes $\boldsymbol{s}$ values (output data) with errors ($\boldsymbol{\epsilon}$) to estimate $\boldsymbol{\theta}$. For nonlinear systems, the linearized system matrix is inserted into the Kalman gain, which is part of the calculation of the prediction value and the covariance. Therefore, Extended Kalman Filter is given by (Kaipio and Somersalo, 2005):

$$K_{k+1} = \frac{P_{k+1}\boldsymbol{\Phi_{k+1}}^{\boldsymbol{T}}}{(\boldsymbol{\epsilon_{k+1}}+\boldsymbol{\Phi_{k+1}}P_k\boldsymbol{\Phi_{k+1}}^{\boldsymbol{T}})} \tag{21}$$

$$\boldsymbol{\theta_{k+1}} = \boldsymbol{\theta_k} + K_{k+1}(\boldsymbol{s_{k+1}} - \boldsymbol{\varphi_{k+1}}(\boldsymbol{\theta_k})) \tag{22}$$

$$P_{k+1} = (1 - K_{k+1}\boldsymbol{\Phi_{k+1}})P_k \tag{23}$$

3 METHODOLOGY

Defined the mathematical model, the coefficients to be identified and identification method to be applied must be obtained observed data to be applied in the method of Extended Kalman Filter and in coupled nonlinear mathematical for rigid multibody.

Data observed in the field correspond to the wind turbine by Enersud, model Verne 555, with tubular tower with tensioned steel cables. These data were analyzed with the purpose of identifying which portions should be selected, since the proposed mathematical model is the assumptions constant direction and speed of the wind.

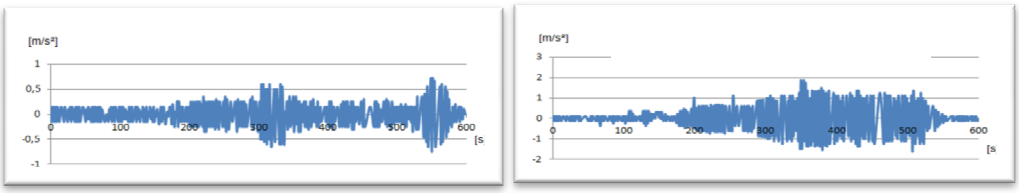

Figure 3 – Observed data for wind tubine time under wind action (Batista, 2009).

As can be seen in figure 3, the mostcritical section corresponds to the interval between 500 and 600 seconds due to its response variable over time deceleration. Data observed in the field correspond only to x and y axis($\hat{n}_1$and $\hat{n}_2$ respectively) related to accelerometers.

For application of the techniques of parameter identification is necessary to make varieties of displacements and velocities in the degrees of freedom considered, since these are the input data. Therefore, it was integrated the accelerations shown in figure 3 for each variation in real time acquired in order to obtain the respective velocities and displacements.

The first page must contain the Title, Author(s), Affiliation(s), Keywords and the Abstract.The second page must begin with the Introduction. The first line of the title is located 3cm fromthe top of the printing box.

Accelerometers were not installed at the ends of the blades for the analysis of these degrees of freedom. For that reason it was considered synthetic data related to the blades, obtained from the reference curves given by the mathematical model here developed, applied values of the stiffness and damping coefficients calculated as literature (Inman, 2001). Above the reference curves were added standard deviations of 0.01 mm for displacement and 0.01 m/s for velocity.

For the simulations, the average wind speed considered was 2 km/h, corresponding 1.16

Hz of rotation frequency, below the natural frequencies of the tower and the blades (tower, flap and lag), according to BATTISTA, 2009.

After obtained displacements and velocities obtained from field data and from synthetic data it is possible to apply the method Extended Kalman Filter to identify stiffness and damping coefficients, using finite differences to approximate the Jacobians of functions, linearizing every moment with a centesimal increment.

Identification process was simultaneous for all coefficients identified totaling ten coefficients identified, two for each degree of freedom. The input data for the identification are the displacements and velocities at each degree of freedom and the output data are the forces due to the acceleration of the system. It was regarded as a model of evolution in each iteration for the parameters identified, namely $\boldsymbol{\theta_{k+1}} = \boldsymbol{\theta_k}$.

Errors were calculated point by point by the following equation:

$$Error = \frac{\|\text{Identified Coefficient} - \text{Reference Coefficient}\|}{\|\text{Reference Coefficient}\|} \; x \; 100\% \qquad (24)$$

Average error refers to the arithmetic mean of all the errors calculated by equation *(24)*. How beaconing quality identification was considered the deviations of ± 2 standard deviations (±2 σ). After parameters identification is possible to apply the coefficients identified in the non-linear mathematical model coupled to rigid multibody here developed, comparing with measure data and reference data.

4 RESULTS

Results of stiffness coefficients identification are shown in figure 4 to 6, for damping coefficients are shown in figure 7 to 9. Results for the blades are shown only for the blade 1, since for other blades the results are very similar.

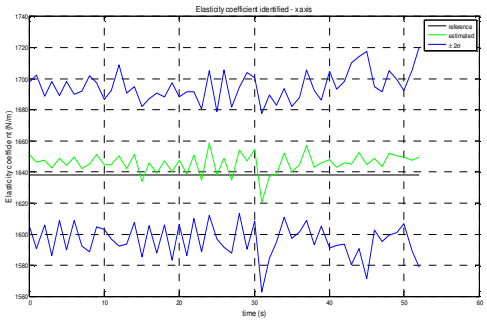

Figure 4 – Stiffness coefficient identification k_x.

In figure 4 it can be seen the dispersion of the data by the change of wind direction between 20 and 40 times. Average error obtained during the identification was 0.23 %.

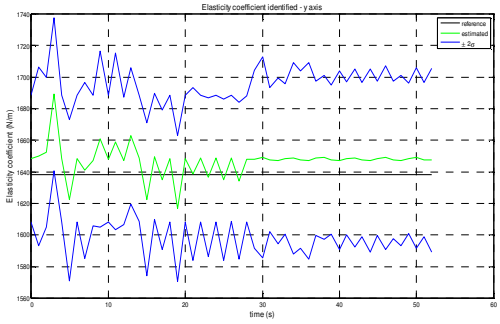

Figure 5 – Stiffness coefficient identification k_y.

In Figure 5 it can see the data dispersion by changing wind direction. Values for the identified coefficient converge to 1650 N/m after 30 seconds, also stabilizing the error. The average error was 0.66 %.

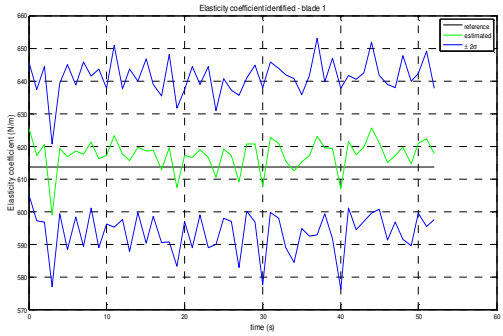

Figure 6 – Stiffness coefficient identification k_{β_1}.

In figure 6 is seen that even than the observed data are synthetic, identification presents itself around a level above the reference value. The average error obtained during the identification was 1.60%.

In figure 7 is possible to agree that, despite the convergence by Extended Kalman Filter identification, this proved to be more sensitive due changing wind direction for identification of the damping coefficient c_x, with a larger amplitudes and average error obtained during the identification, corresponding to 5.41%.

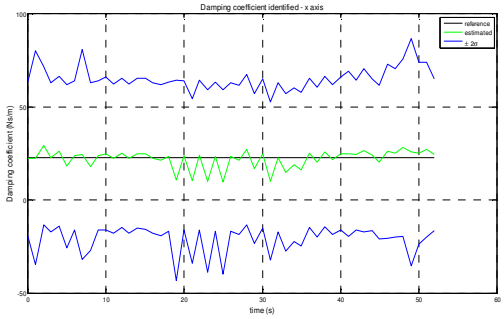

Figure 7 – Damping coefficient identification c_x.

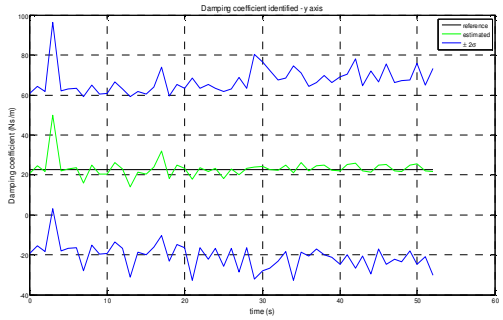

Figure 8 – Damping coefficient identification c_y.

Likewise, in figure 8 shown also a marked error when changing wind direction for identification of damping coefficient c_y. The average error obtained for identification corresponds to 4.53%.

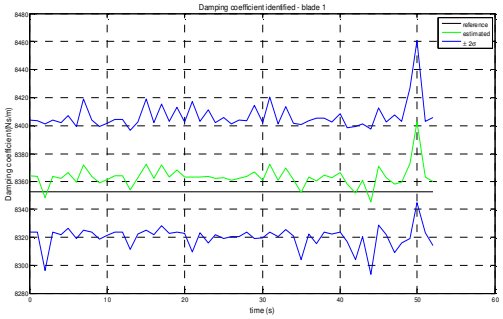

Figure 9 – Damping coefficient identification c_{β_1}.

In figure 9 it notice that the error shown in the identification of damping coefficient c_{β_1} was smaller than in the identification of the other coefficients, according to synthetic data. The average error was 0.01%.

From figure 10 to 12 presents the results using the coefficients identified in the mathematical model considered here or "*model*", compared with the results of "*reference*" and the observed data or "measure". In these results it is possible to see, despite errors in the identification of damping coefficients have been presented with larger magnitudes, the results using the parameters identified in relation to the results of "*reference*" were satisfactory and showed very similar behaviors.

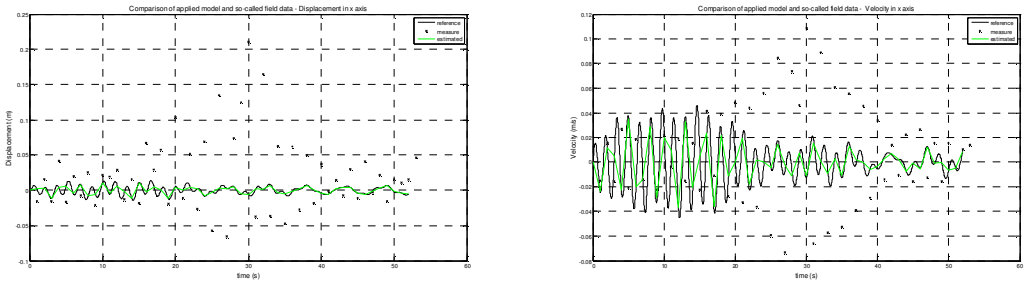

Figure 10 – Displacement and velocity in direction *x*-axis, comparing to the reference and measure data.

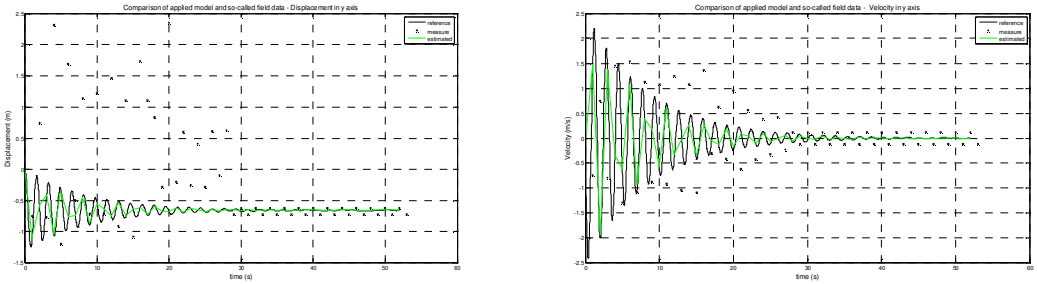

Figure 11 – Displacement and velocity in direction *y*-axis, comparing to the reference and measure data**.**

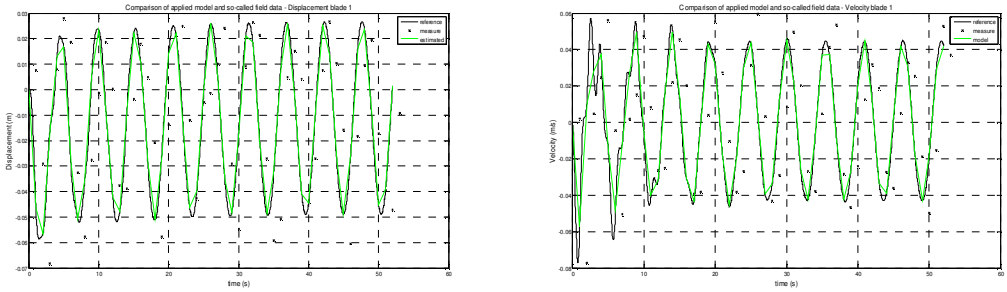

Figure 12 – Displacement and velocity in blade 1, comparing to the reference and measure data**.**

5 CONCLUSIONS

Nonlinear mathematical model proposed by Gonzaga (2013), subsequently applying parameters identification by method Extended Kalman Filter was implemented.

From obtained results it can be seen that the mathematical model here developed showed to be well suited for implementation and easy identification of parameters.

For this application, the Extended Kalman Filter method for parameter identification proved to be very efficient. Horizontal wind turbines have a control system that is possible to smooth wind bursts and over speed winds, turn it non-linearity less severe. Scenarios with other values of the initial conditions were simulated, which are indifferent to the identification. Therefore, it is concluded that we can start the process in any point, making in possible on-line monitoring.

Errors presented by the Extended Kalman Filter method were reasonable, despite showing to be unstable. Just for comparison, it was also identified by SIR Particle Filter method with 2,000 particles. Errors obtained by Extended Kalman Filter method were very similar than those obtained by SIR Particle Filter although unstable. This shows the efficiency of linearization by finite differences with centesimal increase.

The computational cost of the identification by the Extended Kalman Filter method was only 30 seconds and can be applied for online monitoring. Using the same machine that supplied the performance of 30 seconds by the Extended Kalman Filter method, the computational cost for SIR Particle Filter method with 2,000 particles was 103 hours.

Therefore it is concluded that the parameter identification by Extended Kalman Filter method was efficient for the mathematical modeling of the dynamics of three-bladed wind turbines, can be applied in monitoring structural stability and for reducing the costs with field tests for the determination of design parameters.

Future work can be developed by improving the mathematical model developed here, considering the possibility of changing the wind direction and speed, through a stochastic

process. Others methodologies of parameter identification can be also used, like Unscented Kalman Filter method.

REFERENCES

Batista, R., *Aeroelasticidade e controle dinâmico estrutural de turbinas eólicas de eixo horizontal*. Relatório Técnico, projeto CNPq. Universidade Federal do Rio de Janeiro. Rio de Janeiro, RJ, Brasil, 2009.

Edenhofer, O., *Renewable Energy Sources and Climate Change Mitigation*. Intergovernmental Panel on Climate Change (IPCC). Cambridge University Press, 2011.

Flowers, G. T., and Tongue, B. H., Nonlinear Rotorcraft Analysis using Symbolic Manipulation. *International Journal of Nonlinear Mechanics*, 23(3):154-160, 1998.

Gonzaga, F. G., *Modelos Computacionais para Análise da Vibração Acoplada Rotor-Pás com Aplicação em Turbinas Eólicas e Ressonância de Solo de Helicópteros*. Projeto de Graduação, Universidade Federal do Rio de Janeiro. Rio de Janeiro, RJ, Brasil, 2013.

Inman, D. J., *Engineering Vibration. International Edition*, 2ª ed. Prentice Hall International Inc, 2011.

Kaipio, J., and Somersalo, E., *Statistical and Computational Inverse Problems*, 1ª ed. Springer Science and Business Media Inc, 2004.

Ristic, B., and Arulampalam, S., and Gordon, N., *Beyond the Kalman Filter:Particle Filters for Tracking Applications*. Artech House Radar Library, 2004.

Robinson, C. S., *Modeling and analysis of helicopter ground resonance utilizing symbolic processing and dynamic simulation software*. Tese de Doutorado. Escola de Pós-Graduação Naval. Monterey, CA, EUA, 1997.

Saracho, C. M., *Modelos matemáticos lineares e não-lineares para representar o acoplamento entre rotor e palhetas flexíveis - exemplos numéricos e verificação experimental*. Tese de Doutorado. Universidade Estadual de Campinas. Campinas, SP, Brasil, 2002.

Tenenbaum, R., *Dinâmica aplicada*, 3ª ed. EditoraManole, 2006.